
Wavelet transform and mel-frequency cepstral coefficient-based feature extraction of the sheet metal trimming process to study burr formation

Tushar Y. Badgujar* and Vijay P. Wani

Mechanical Engineering Department,
Mumbai Educational Trust's Institute of Engineering,
Affiliated to Savitribai Phule Pune University,
Nashik, Maharashtra, 422003, India
Email: tybadgujar@gmail.com
Email: vpwani@rediffmail.com
*Corresponding author

Abstract: The sheet metal trimming process is extensively employed to achieve the final shape of components. However, burr formation is a major quality related issue of trimmed parts, and the burr height could be utilised to assess the quality of the component. Punch wear and material thickness variation were considered significant parameters, causing deviation in the burr height. This study proposes the pragmatism of the wavelet transform (WT) coupled with mel-frequency cepstral coefficients (MFCCs) to extract acoustic signal features to examine burr formation. The MFCCs of features indicate variations in the process parameters. Furthermore, the experimental results reveal a correlation between burr formation and MFCCs. These results suggest that the WT, coupled with MFCCs, can be useful in retrieving features pointing burr formation. Thus, features of the signal could be used to monitor the burr height, and these would prevent the need for offline burr height measurement, reworking, and scrapping.

Keywords: sheet metal trimming; MFCCs; mel-frequency cepstral coefficients; acoustic emission; feature extraction; monitoring.

Reference to this paper should be made as follows: Badgujar, T.Y. and Wani, V.P. (2022) 'Wavelet transform and mel-frequency cepstral coefficient-based feature extraction of the sheet metal trimming process to study burr formation', *Int. J. Mechatronics and Manufacturing Systems*, Vol. 15, No. 1, pp.20–36.

Biographical notes: Tushar Y. Badgujar is a Research Scholar and pursuing his PhD at the MET's IOE, Bhujbal Knowledge City, Nashik under SPPU, Pune. He obtained his Master's from the Rajiv Gandhi Proudyogiki Vishwavidyalaya, Bhopal and Bachelor's from the North Maharashtra University, India. His areas of research are sheet metal forming, signal processing and machine condition monitoring and improvement in decision making by integrating interdisciplinary engineering knowledge.

Vijay P. Wani is working as the Principal at the MET's IOE, Bhujbal Knowledge City, Nashik, India. He received his PhD and Master's in Mechanical Engineering from the NIT, Kurukshetra, India. More than

10 students completed and four students are undergoing PhD course under his supervision. In his credit, more than 30 papers are published in national and international journal and around 40 papers in conferences.

1 Introduction

The stamping process is utilised in several industries, such as the automotive, aerospace, and household appliance industries, for manufacturing various components (Hambli, 2002; Ge et al., 2004; Li and Bassiuny, 2008). The components are mainly produced using two mechanisms, namely, deformation and shearing (Ge et al., 2008). Sheet metal processes such as blanking, punching, and trimming involve shearing of the sheet metal to achieve the desired shape. In the case of the sheet metal trimming process, the excess portion of the component is removed using a punch and die. The sheet metal trimming process involves a series of phases (Bassiuny et al., 2007). The trimming is initiated by establishing contact between the tool and the sheet metal. The tool start exerting pressure on the sheet and deforms it elastically. As the pressure on the sheet reaches its yield strength, the sheet gets deformed like a plastic material. When pressure at the cutting edge on the sheet increases, and reaches shear strength of the sheet, it results in trimming of excess material. The trimmed edge of sheet consists of the rollover zone, shear zone, fracture zone, and the burr (Hilditch and Hodgson, 2005). Generally, a trimmed edge with a large shear zone and a small burr is preferred. Punch die clearance and punch wear are considered as the major factors affecting the formation of the burr. In sheet metal trimming processes, one seeks to generate cracks at the sharp edges of the punch and the die; the cracks need to be propagated as soon as possible to obtain total rupture. Punch wear causes the cutting edges to be rounded and changes the punch-die geometry and clearance. With the increase in wear, the radius of the rounding increases, which, in turn, decreases the sharpness of the punch. This decrease in sharpness influences the sheared zone of the trimming edge and increases the deformation of workpiece. Furthermore, the fracture zone and the burr of the part become larger. The punch penetration corresponding to the crack's initiation in the sheet increases, which degrades the surface finish of the product. Additionally, the noise level of the press and the force required to accomplish the process increase (Hambli, 2002; Hambli and Guerin, 2003). As it is difficult to measure the burr height on the shop floor, the online condition monitoring technique becomes important for understanding the burr height variation. Apart from acoustic signals, various other signals are used for monitoring the conditions in the stamping process (Badgujar and Wani, 2019). Acoustic emission (AE) occurs during the process in the form of short-lived stress waves because of material deformation, crack development, crack propagation, and fracture. In acoustic measurement, A transducer (microphone) acoustically coupled to a source undergoing dynamic changes, detects the elastic (acoustic) emitted energy and gives information about the dynamic changes taking place. Microphones sense small changes in sound pressure through the motion of a thin diaphragm. All microphones consist of a diaphragm that moves back and forth in response to changes in pressure or velocity brought about by an acoustic emission and then the movement of diaphragm is converted into an electric signal. Microphone is selected based on requirements such as sensitivity, frequency response and directionality. Fundamentally, AE testing system consists of a microphone/sensor, amplifier with

appropriate filters, analogue to digital convertor, data acquisition system and computer with the digital signal processing facility (Baccar and Soffker, 2015; Badgajar and Wani, 2019).

Wavelet transform (WT) can exhibit localised properties in both domains (Baccar and Soffker, 2015), and is suitable for acoustic signal processing (Bianchi et al., 2015). The WT replaces the signal based on finite basis functions. When employing the WT, the transient characteristics can be revealed by measuring the amount of decay of the wavelet function (Zhu et al., 2009; Niaki et al., 2016). Using the acoustic signal, an expert operator can differentiate between various parameter changes using the normal human hearing ability. As a result, acoustic signals are naturally used for machine condition monitoring. The mel-frequency cepstral coefficient (MFCC) is a signal processing technique that imitates the natural process whereby humans process audio signals. It was initially used for speech processing. However, eventually, various researchers discovered and justified the use of MFCCs for monitoring aspects such as machine condition, heart condition, and structural analysis (Frigieri et al., 2016; Mei et al., 2019; Deng et al., 2020; Liu et al., 2020). The MFCC has time–frequency information and is a two-dimensional feature. It reflects the non-steady state characteristics of the sound signal. Through the study of the human earing, it is found that the hearing sensitivity of the human ear for different frequencies of sound waves is greatly different. Mel scale describes the non-linear characteristics of human ear frequency perception, and its approximate expression with linear frequency. Based on the Mel frequency, various researcher designed a series of triangular filter banks from low frequency to high frequency to filter the input sound signal. The signal energy output by each filter is used as the basic feature. After subsequent processing, the MFCC feature vector is obtained. In this study, 24 MFCCs were extracted from the acquired acoustic signal and used as features to discriminate among variations in the parameters and burr height (Zhai et al., 2015; Frigieri et al., 2016; Liu et al., 2020; Jin et al., 2021).

Burr formation is a prominent defect related to sheet metal trimming and restricting the height of the burr is a major manufacturing concern. The burr is formed during all shearing and cutting operations of sheet metal, such as blanking, trimming, and punching (Picart et al., 2008). Its formation is inevitable in the case of trimmed parts; however, when a specified limit is exceeded, the burr becomes a defect. Excessive burr formation leads to issues related to product quality and the need for rework. Thus, controlling the formation of this defect is critical. Researchers regard punch-die clearance as an essential influencing factor for burr development (Husson et al., 2008; Akyürek et al., 2017). The clearance value changes with variations in the die dimension, punch dimension, or the thickness of the sheet. Moreover, researchers even believe that the punch wear is among the major influencing factors that change the punch geometry and affect burr formation (Hambli, 2002; Akyürek et al., 2017).

Currently, the sheet metal trimming process is used in the mass-production of components. It involves the use of a long metal sheet as the raw material. These sheets are produced using a rolling process, wherein variations in the thickness of the sheet are evident. Furthermore, in some cases, it is necessary to change the thickness of the sheet because of changes in design. The subsequent changes in the thickness of the sheet are bound to modify the relationship between the punch-die clearance. Variations in the material thickness are witnessed abruptly when all the other parameters remain unchanged. This phenomenon creates the need to conduct this study to understand the relationship among variations in material thickness, punch wear, clearance, and burr

formation. Meanwhile, feature extraction is necessary for monitoring the condition of the system to study variations in burr height. This study aims to

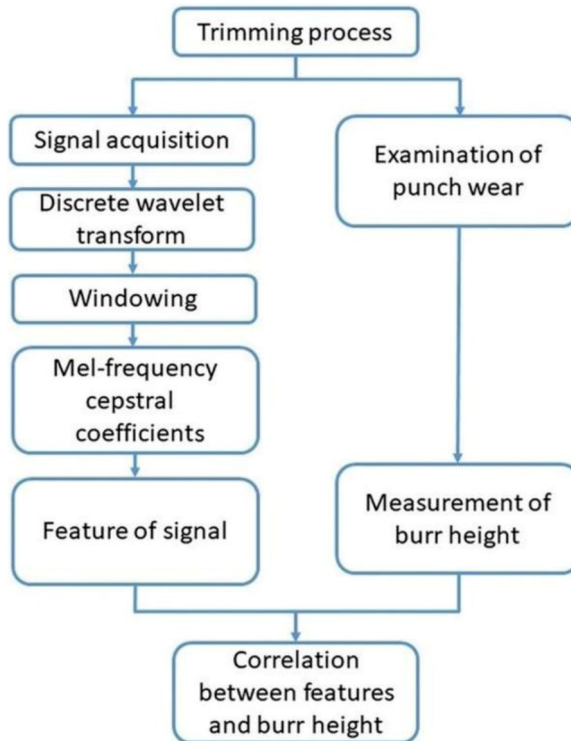
- 1 investigate the effect of sheet thickness variation and punch wear on burr formation
- 2 extract acoustic signal features during the sheet metal trimming process to study burr formation.

In this study, use of the WT at the initial stage eliminates the unwanted frequencies from the signal and improves the MFCC's feature extraction accuracy. The correlation between the features, parameter variation, and burr height indicates the possibility of utilising the proposed methodology for burr height prediction.

2 Methodology

Figure 1 illustrates the methodology followed in this study. First, the discrete WT was utilised to replace the acoustic signals. Second, the windowing approach was used over the transformed signals to slice them. Next, the mel-cepstral coefficients were evaluated from the windowed acoustic signal. Finally, a correlation was established between features and burr height.

Figure 1 Workflow (see online version for colours)



3 Experiments

3.1 Experimental setup

In the experimental setup, a radial tyre valve protector was used as a research object. Tyre valve protectors are used in heavy-duty vehicles, such as trucks and tractors. Owing to the large size of such valves, nuts cannot be used as valve protectors. To meet the high market demand for them, these tyre valves are produced in large quantities every year. Burr formation, fracture, and wrinkling are the main defects observed during the production of such valves. Figure 2 shows an actual image of a tyre valve protector. Table 1 lists the material properties (Bureau of Indian Standard, 2008).

Figure 2 Radial tyre valve protector (see online version for colours)



Table 1 Material properties

| <i>S. no.</i> | <i>Description</i> | <i>Details</i> |
|---------------|--------------------------|------------------------------|
| 1 | Material type | Cold rolled close annealed |
| 2 | Grade | CR4 – Extra deep drawn (EDD) |
| 3 | Designed sheet thickness | 1.00 mm |
| 4 | Tensile strength | 350 MPa (Max.) |

The component was produced from a metal sheet. It underwent various stamping processes before being modelled into its final geometry via the trimming process. This study largely focused on the sheet metal trimming operation. Figure 3 illustrates the trimming operation of a radial tyre valve protector.

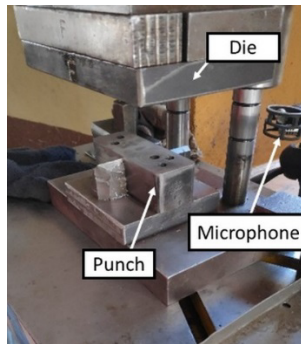
In this study, the trials were conducted on a C-type, 20-ton mechanical power press (RCP-20, Rajesh Machines (India) LLP, Rajkot, India). For performing the sheet metal trimming operation, the die and punch arrangement was set up as shown in Figure 4. The dimensions of the punch and the die were decided considering the designed sheet thickness of 1.00 mm and the 5% clearance of sheet thickness between the punch and the die. The dimensions of the punch and the die were maintained unchanged throughout the

experiment. Three levels of punch wear were considered for the experiments, namely, a freshly ground punch, partially worn punch (i.e., when the height of the burr reaches 10% for a sheet thickness of 1.00 mm), and fully worn punch (i.e., when the height of the burr reaches up to approximately 15% for a sheet thickness of 1.00 mm). Meanwhile, the respective sheet thickness sizes considered for this study were 0.8, 0.9, 0.93, 0.97, 1.00, 1.03, 1.05, 1.10, and 1.20 mm. Accordingly, for each thickness and punch condition combination, 20 components were trimmed. A microphone (Zoom H1/MB) was positioned at 150 mm from the die to record the acoustic signal of the sheet metal trimming process.

Figure 3 Component (a) before and (b) after the sheet metal trimming process (see online version for colours)



Figure 4 Experimental setup (see online version for colours)



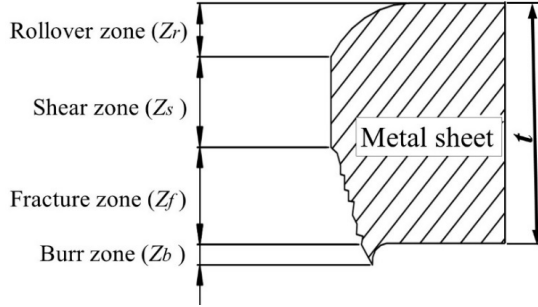
A triggering circuit control based on a proximity sensor was used to capture the interval signal. Following this arrangement, experiments were performed for 27 combinations (nine sheet thicknesses and three punch wear conditions). For each combination, 20 components were produced, and subsequently, 540 test signals were collected.

3.2 Measurements

Random trials were performed for various thickness and punch wear combinations and the burr height for each component was assessed using a vision measuring system (VMS) (Rapid-I, Customised Technologies (P) Ltd., Bengaluru, India). The VMS magnifies the

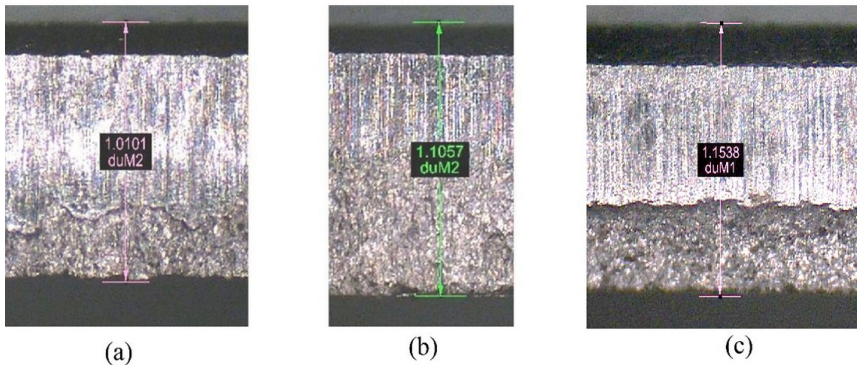
image at a resolution power of 67X and measures the distance. It is a contactless measuring equipment with a least count of 0.0001 mm. Figure 5 illustrates the geometry of the trimmed edge.

Figure 5 Geometry of the trimmed edge



In Figure 5, the cross section of the sheet shows four zones, namely, rollover zone (Z_r), shear zone (Z_s), fracture zone (Z_f) and burr zone (Z_b), while t is the sheet thickness. Figure 6 shows the respective images of the trimmed edges for the three punch conditions (i.e., freshly ground punch, partially worn punch, and fully worn punch) studied using a 1.00 mm-thick sheet.

Figure 6 Burr height for a 1.00 mm thick sheet for (a) freshly ground punch, (b) partially worn punch, and (c) fully worn punch. The values 1.0101, 1.1057, and 1.1538 represent the sum $Z_r + Z_s + Z_f + Z_b$ in mm for the particular punch (see online version for colours)



The burr height was evaluated using the following equation (Zhai et al., 2015):

$$\text{Burr zone } (Z_b) \text{ or Burr height} = (Z_r + Z_s + Z_f + Z_b) - t \tag{1}$$

3.3 Feature extraction

During trials, the acoustic signals were recorded. The experiments were performed at various parameter levels. Generally, one cycle/stroke of sheet metal trimming operations consists of the following sequential events:

- 1 the downward movement of the die until the sheet holder touches the sheet
- 2 the downward movement of the die to perform the cutting process
- 3 the upward movement of the die to its original position.

Typically, a time domain signature of the punching process involves this sequence of events. However, during this study, the signal processing complexity was significantly reduced by the triggering circuit, and the signal related to the cutting operation was captured. The acoustic signals were recorded using a microphone at a sampling rate of 44,100 Hz. The corresponding signals were processed using MATLAB R2020a prepared code.

Figure 7 depicts the continuously recorded signal. The peak indicates the trimming process. It was observed that there was silence between two consecutive peaks when the triggering circuit was off. Figure 8 represents the individual process audio signal.

Figure 7 Recorded signal for a continuous process (see online version for colours)

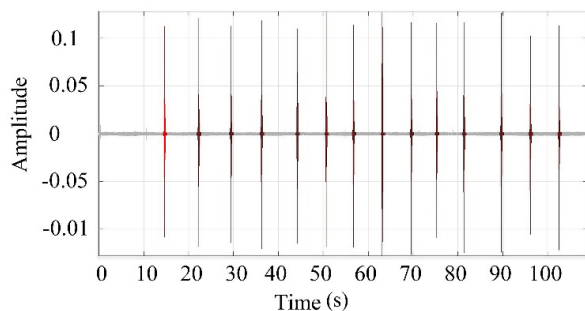
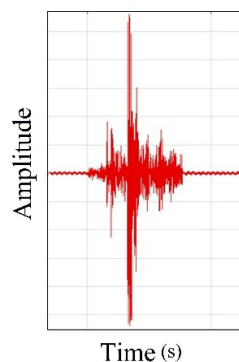


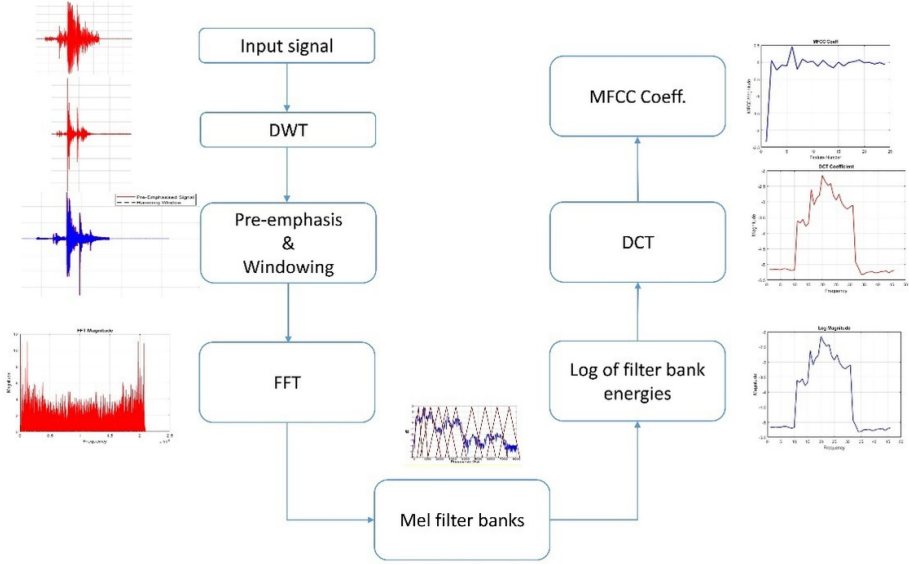
Figure 8 Individual process signal (see online version for colours)



The acoustic signal is decomposed using the discrete wavelet transform (DWT). The symmlet wavelet is utilised to represent the signal up to eight levels. The symmlet wavelet family is deemed suitable for the analysis, considering its effectiveness in denoising similar signals. The energy distribution of the reconstructed wavelet coefficients was based on the distribution of the multi-resolution frequency bands, and it was used as an input to MFCC. MFCC initially determined the different frequency components, and, in the later stages, it determined the spectrum to identify the MFCCs.

The extraction of MFCCs is performed to obtain the MFCC value of the approximate wavelet coefficients. A total of 31 band filters were used, of which 13 were linear filters and 18 were log filters. Figure 9 outlines the general steps followed during feature extraction (Frigieri et al., 2016).

Figure 9 Feature extraction (see online version for colours)



The procedure to evaluate the MFCCs can be summarised as follows:

- i The pre-emphasis filter boosts the amount of energy across high frequencies of the signal. The boosting of energy makes information in higher formats available for further analysis.
- ii After pre-emphasis, the signal is sliced in short time frames. The slicing of the signal can lead to an addition in the noise due to the sudden drop in amplitude. In this study, the Hamming window is used as it reduces the spectral distortion by shrinking the beginning and end of each frame of the signal to zero. This is expressed as follows:

$$w(n) = 0.54 - 0.46 \cos\left(\frac{2\pi n}{F-1}\right), \quad 0 \leq n \leq F-1 \tag{2}$$

where F is the frame size.

The energy spectrum of the signal is then calculated using the discrete Fourier transform, which is expressed as

$$X_k = \sum_{n=0}^{N-1} \tilde{X}_k(n) e^{2\pi kn/N} \tag{3}$$

$$S_k = |X_k|^2 \tag{4}$$

where X_k denotes the discrete Fourier transform, S_k is the spectral energy, and N denotes the number of fast Fourier transform (FFT) points. The spectrum is rich in information, wherein the triangular band pass filter maps measured frequencies with respect to the mel-frequency scale. The mel scale filter bank is utilised to obtain the mel scale power spectrum. The output of the mel scale power spectrum represents the energy of the various frequency bands.

iii In the last stage, the discrete cosine transform (DCT) is applied to extract the MFCC feature. Accordingly, the filter bank coefficient derives a compressed illustration of the filter bank, which is expressed as

$$C_k(m) = \sum_{l=0}^{L-1} \log(\tilde{S}_k(l)) \cos\left(\frac{\pi m}{2L}(2l+1)\right), \quad \forall k=1, \dots, K \quad (5)$$

where $m = 1, 2, \dots, C$; C denotes the number of desired coefficients.

Figures 10–12 illustrate the MFCCs for the 27 combinations.

Figure 10 MFCCs of sheets based on their thickness, using freshly ground punch: (a) 0.8 mm; (b) 0.9 mm; (c) 0.93 mm; (d) 0.97 mm; (e) 1.00 mm; (f) 1.03 mm; (g) 1.05 mm; (h) 1.10 mm and (i) 1.20 mm (see online version for colours)

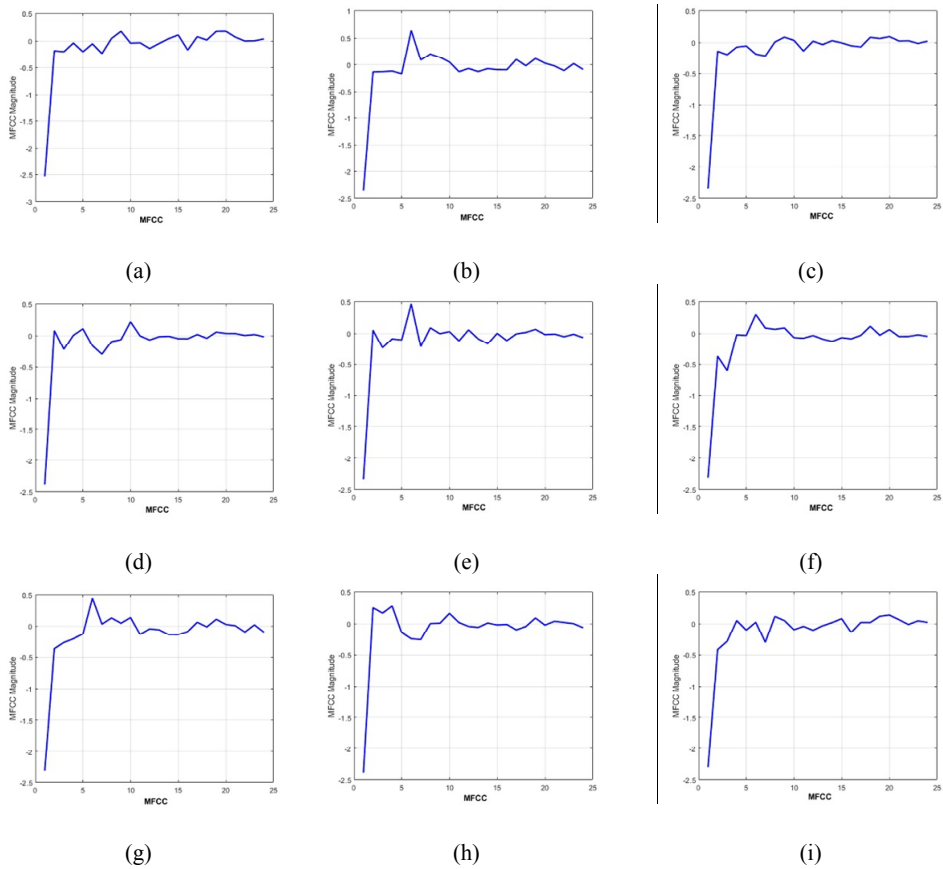
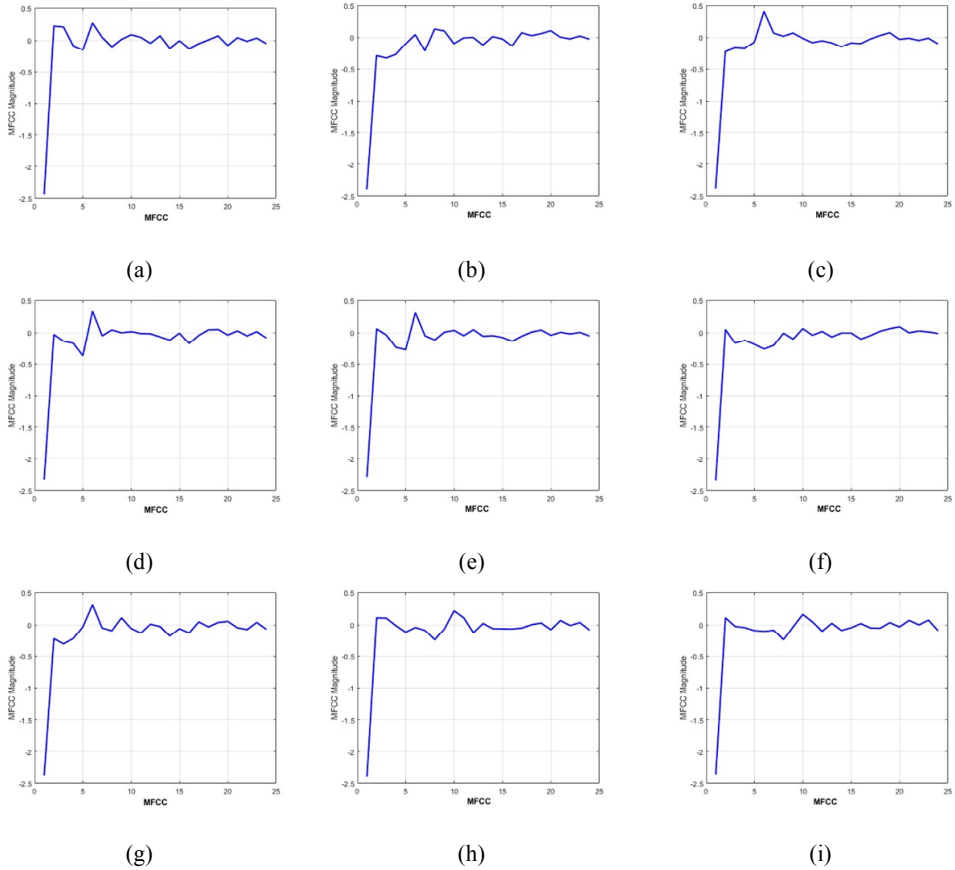


Figure 11 MFCCs of sheets based on their thickness, using partially worn punch: (a) 0.8 mm; (b) 0.9 mm; (c) 0.93 mm; (d) 0.97 mm; (e) 1.00 mm; (f) 1.03 mm; (g) 1.05 mm; (h) 1.10 mm and (i) 1.20 mm (see online version for colours)



4 Results and discussion

The burr height of experimental objects was evaluated, and the average burr heights for various punch conditions and sheet thicknesses are given in Table 2. For the freshly ground punch, the burr height was observed to be well below the permissible limit for all sheet thicknesses. However, the results indicate that the prediction of burr formation becomes challenging with the increase in punch wear. As the sheet thickness decreased below 1.00 mm, the burr height increased.

Figure 12 MFCCs of sheets based on their thickness, using fully worn punch: (a) 0.8 mm; (b) 0.9 mm; (c) 0.93 mm; (d) 0.97 mm; (e) 1.00 mm; (f) 1.03 mm; (g) 1.05 mm; (h) 1.10 mm and (i) 1.20 mm (see online version for colours)

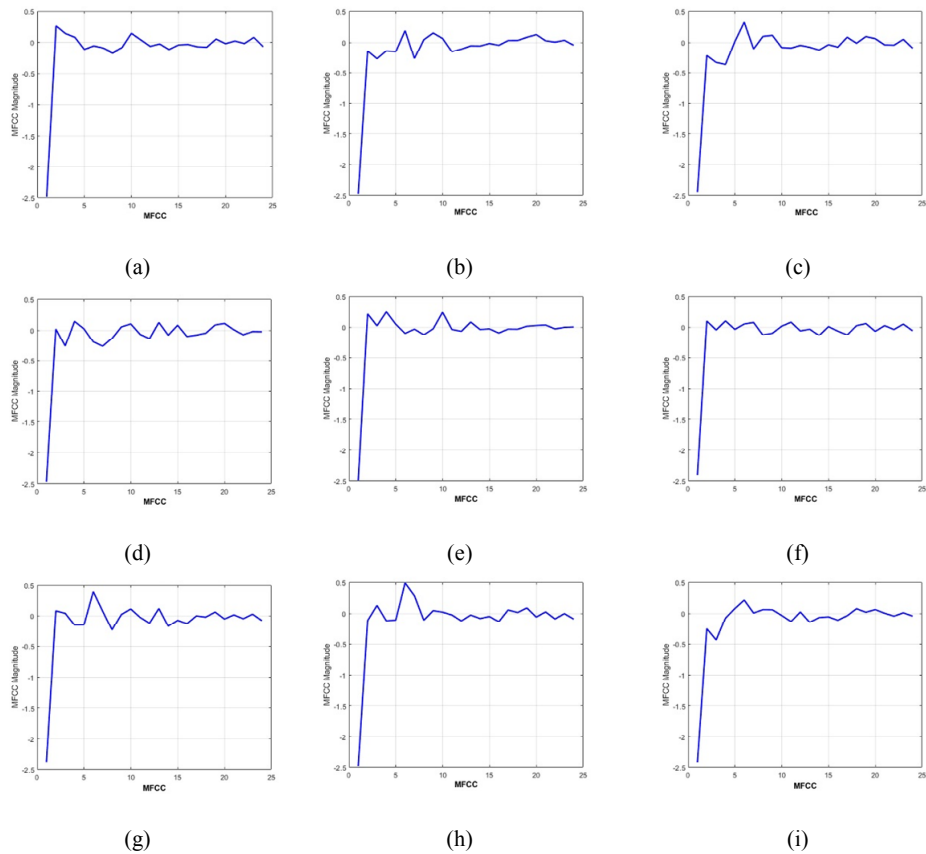


Table 2 Measured burr heights (mm)

| Sheet thickness | Punch type | | |
|-----------------|------------|----------|----------|
| | <i>S</i> | <i>P</i> | <i>B</i> |
| 0.80 | 0.0685 | 0.1350 | 0.2014 |
| 0.90 | 0.0319 | 0.1342 | 0.1768 |
| 0.93 | 0.0162 | 0.1304 | 0.1735 |
| 0.97 | 0.0153 | 0.1312 | 0.1725 |
| 1.00 | 0.0135 | 0.1082 | 0.1685 |
| 1.03 | 0.0126 | 0.0979 | 0.1285 |
| 1.05 | 0.0138 | 0.0938 | 0.1064 |
| 1.10 | 0.0092 | 0.1025 | 0.1128 |
| 1.20 | 0.0062 | 0.0974 | 0.1200 |

S, P, and B denote freshly ground, partially worn, and fully worn, respectively.

Thus, burr height growth is associated with punch wear and clearance. Continuation of the production resulted in wear and made the trimming edge of punch blunt. It is also observed that the blunt cutting edge resulted in the production of components with greater burr height. During the study, for a sheet thickness of 1.00 mm, the punch-die clearance on each side was considered to be 5%. With a decrease in thickness, both the actual clearance and the burr height of the component increased. Conversely, the burr height decreased gradually with an increase in sheet thickness. Figure 13 shows deviation of actual clearance from the required clearance. The percentage burr height vs. sheet thickness was plotted for different punch conditions, as shown in Figure 14.

Figure 13 Clearance variation (see online version for colours)

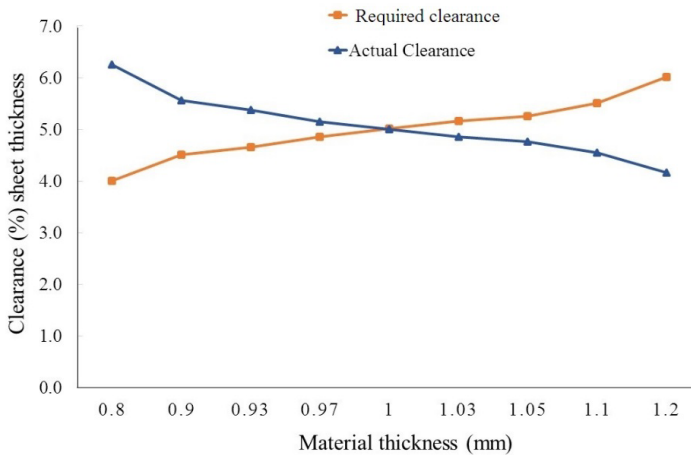
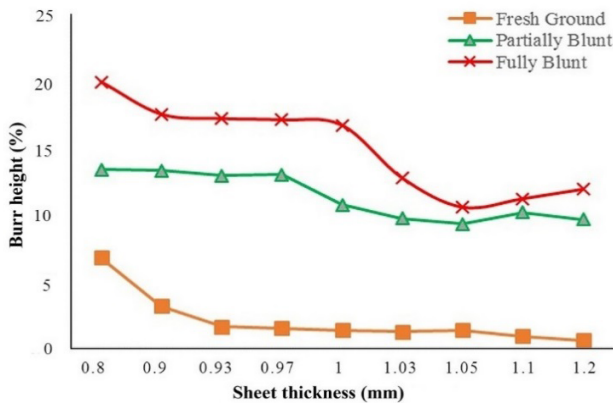


Figure 14 Burr height variation (see online version for colours)

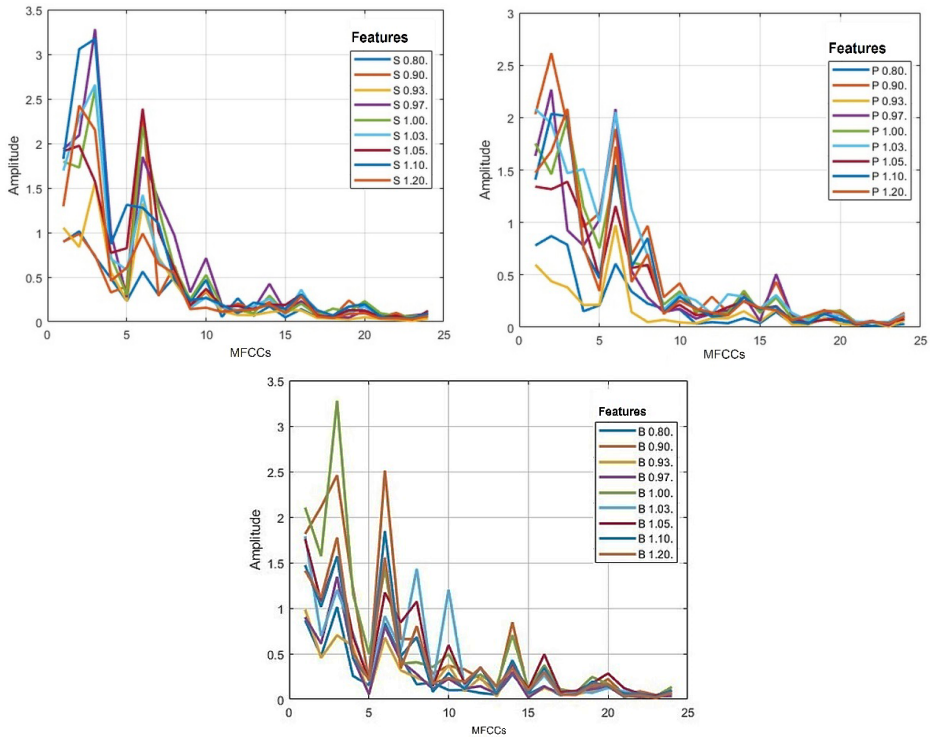


These signals included components such as trimming process signal, surrounding noise, and machine noise. Meanwhile, relevant information related to the variation in parameters could not be obtained with the help of the time domain signal. Moreover, the WT and MFCC utilise the time-frequency domain to analyse the signal and are more advantageous over other processing methods involving the use of the frequency domain signal.

The MFCCs represent changes in the signal at various stages and mark the signal features. The 24 MFCC values of the individual sound signal of the sheet metal trimming process identify the feature for the combination of parameters and burr height. The 27 features for the 27 experimental conditions are shown in Figure 15. Even in the case of sheets with the same thickness, the comparison between the features extracted for different punch conditions, namely freshly ground (S), partially worn (P), and fully worn (B), shows a clear distinction.

Figure 15 outlines the sheet features for all punch wear conditions according to the thicknesses.

Figure 15 Sheet features for different punch wear states. S, P, and B denote freshly ground, partially worn, and fully worn, respectively (see online version for colours)



A Pearson correlation coefficient analysis reveals that a strong correlation exists between the features and burr formation. From Tables 2 and 3, the correlation between the feature value and burr height is established.

The study reveals that MFCC numbers 3 and 12 of the freshly ground punch exhibit a strong correlation with the burr height. Further, MFCC numbers 11 and 15 of the partially worn punch show a strong correlation with burr height, and MFCC numbers 8, 12, and 16 of the fully worn punch exhibit a strong correlation with the burr height. The correlation between MFCCs and the burr height is significant because the 24 MFCCs define the feature of the sound signal. The features of the 27 experimental conditions identify the burr height listed in Table 2. Table 4 presents the correlation between the sheet thickness and feature value. It is evident that for the freshly ground punch, MFCC numbers 2 and

16 exhibit a strong correlation with the sheet thickness variation. Similarly, in the case of the partially worn punch, MFCC number 15 shows a strong correlation with the thickness variation, whereas in the case of the fully worn punch, MFCC number 12 shows a strong correlation with the thickness variation.

Table 3 Correlation between average burr height and MFCC amplitude (feature)

| Punch type | S | | P | | B | | |
|-------------------------------|---------|--------|---------|---------|---------|---------|---------|
| MFCC No./Sheet Thickness (mm) | 3 | 12 | 11 | 15 | 8 | 12 | 16 |
| 0.80 | 0.7297 | 0.2633 | 0.0343 | 0.0396 | 0.1643 | 0.0693 | 0.1429 |
| 0.90 | 0.7402 | 0.2057 | 0.1340 | 0.1389 | 0.6591 | 0.2264 | 0.2978 |
| 0.93 | 1.5630 | 0.0758 | 0.0370 | 0.0564 | 0.2387 | 0.2405 | 0.1232 |
| 0.97 | 3.2812 | 0.1071 | 0.0819 | 0.0588 | 0.2759 | 0.1434 | 0.1405 |
| 1.00 | 2.6066 | 0.1314 | 0.1560 | 0.1379 | 0.4067 | 0.2720 | 0.3738 |
| 1.03 | 2.6564 | 0.1319 | 0.2558 | 0.1786 | 1.4310 | 0.3450 | 0.2628 |
| 1.05 | 1.5717 | 0.1762 | 0.1153 | 0.1746 | 1.0732 | 0.3507 | 0.4940 |
| 1.10 | 3.1715 | 0.0969 | 0.1835 | 0.1723 | 0.6831 | 0.3532 | 0.3434 |
| 1.20 | 2.1491 | 0.1283 | 0.1770 | 0.1863 | 0.8026 | 0.3470 | 0.2956 |
| <i>r</i> | -0.6904 | 0.8406 | -0.7355 | -0.8675 | -0.7650 | -0.9089 | -0.6905 |
| <i>p</i> | 0.0395 | 0.0045 | 0.0239 | 0.0024 | 0.0163 | 0.0007 | 0.0395 |

S, P, and B denote freshly ground, partially worn, and fully worn, respectively and P-value < 5% is considered as significant for two-tail tests.

Table 4 Correlation between sheet thickness and MFCC amplitude (Feature)

| Punch type | S | | P | B |
|-------------------------------|--------|--------|--------|--------|
| MFCC No./sheet thickness (mm) | 2 | 16 | 15 | 12 |
| 0.80 | 1.0153 | 0.1414 | 0.0396 | 0.0693 |
| 0.90 | 0.9838 | 0.2065 | 0.1389 | 0.2264 |
| 0.93 | 0.8373 | 0.1274 | 0.0564 | 0.2405 |
| 0.97 | 2.0898 | 0.2309 | 0.0588 | 0.1434 |
| 1.00 | 1.7289 | 0.2032 | 0.1379 | 0.2720 |
| 1.03 | 2.2941 | 0.3590 | 0.1786 | 0.3450 |
| 1.05 | 1.9740 | 0.3068 | 0.1746 | 0.3507 |
| 1.10 | 3.0567 | 0.3073 | 0.1723 | 0.3532 |
| 1.20 | 2.4243 | 0.2845 | 0.1863 | 0.3470 |
| <i>r</i> | 0.812 | 0.727 | 0.788 | 0.841 |
| <i>p</i> | 0.008 | 0.026 | 0.012 | 0.005 |

S, P, and B denote freshly ground, partially worn, and fully worn, respectively and P-value < 5% is considered as significant for two-tail tests.

5 Conclusion

In this study, an acoustic-based monitoring method was developed for the sheet metal trimming process. The variations in the material thickness and punch wear states are important parameters influencing the burr height, which was confirmed through actual burr height measurement. A model comprising a WT, coupled with MFCC, was used to derive features from the signal. The features for the parameter combinations were defined by 24 MFCCs values, and each feature remained distinct as the thickness and punch wear states were varied. The correlation analysis indicated the existence of correlation between the features and burr height. Online extraction of features from new process signals and a comparison with 27 existing features enabled the prediction of the burr height and the parameter level. A suitable classifier capable of comparing 24 MFCCs values with 27 existing features is required for predicting the burr height. The increase in sheet thickness and lesser punch wear resulted in decreased burr height. The proposed methodology may be used for transient sheet metal operations such as blanking, punching, and trimming in which shearing of sheet metal occurs on the mechanical press. However, in a real-world factory environment, multiple machines operate, which inhibits the process of capturing individual acoustic signals. Furthermore, more than one MFCC correlates with the burr formation and parameters; therefore, a classifier capable of comparing multiple values simultaneously is required for studying parameter variations and burr prediction. The use of unidirectional microphones and sound isolation between machines could reduce the noise in signals.

References

- Akyurek, F., Yaman, K. and Tekiner, Z. (2017) 'An experimental work on tool wear affected by die clearance and punch hardness', *Arabian Journal for Science and Engineering*, Vol. 42, No. 11, pp.4683–4692.
- Baccar, D. and Soffker, D. (2015) 'Wear detection by means of wavelet-based acoustic emission analysis', *Mechanical Systems and Signal Processing*, Vols. 60–61, pp.198–207.
- Badgujar, T.Y. and Wani, V.P. (2019) 'Performance study of stamping process using condition monitoring: a review', *Proceedings of International Conference on Intelligent Manufacturing and Automation, Lecture Notes in Mechanical Engineering*, Mumbai, Maharashtra, India, pp.521–529.
- Bassiuny, A.M., Li, X. and Du, R. (2007) 'Fault diagnosis of stamping process based on empirical mode decomposition and learning vector quantization', *International Journal of Machine Tools and Manufacture*, Vol. 47, No. 15, pp.2298–2306.
- Bianchi, D., Mayrhofer, E., Groschl, M., Betz, G. and Vernes, A. (2015) 'Wavelet packet transform for detection of single events in acoustic emission signals', *Mechanical Systems and Signal Processing*, Vols. 64–65, pp.441–451.
- Bureau of Indian Standard (2008) *IS 513: 2008 Cold Reduced Low Carbon Steel Sheets and Strips [MTD 4: Wrought Steel Products]*, pp.1–10, Available at: www.bis.org.in
- Deng, M., Meng, T., Cao, J. Wang, S., Zhang, J. and Fan, H. (2020) 'Heart sound classification based on improved MFCC features and convolutional recurrent neural networks', *Neural Networks*, Vol. 130, pp.22–32.
- Frigieri, E.P., Campos, P.H.S., Paiva, A.P., Balestrassi, P.P., Ferreira, J.R. and Ynoguti, C.A. (2016) 'A mel-frequency cepstral coefficient-based approach for surface roughness diagnosis in hard turning using acoustic signals and Gaussian mixture models', *Applied Acoustics*, Vol. 113, pp.230–237.

- Ge, M., Xu, Y. and Du, R. (2008) 'An intelligent online monitoring and diagnostic system for manufacturing automation', *IEEE Transactions on Automation Science and Engineering*, Vol. 5, No. 1, pp.127–139.
- Ge, M., Du, R. and Xu, Y. (2004) 'Hidden markov model based fault diagnosis for stamping processes', *Mechanical Systems and Signal Processing*, Vol. 18, No. 2, pp.391–408.
- Hambli, R. (2002) 'Design of experiment based analysis for sheet metal blanking processes optimisation', *International Journal of Advanced Manufacturing Technology*, Vol. 19, No. 6, pp.403–410.
- Hambli, R. and Guerin, F. (2003) 'Application of a neural network for optimum clearance prediction in sheet metal blanking processes', *Finite Elements in Analysis and Design*, Vol. 39, No. 11, pp.1039–1052.
- Hambli, R. (2002) 'Prediction of burr height formation in blanking processes using neural network', *International Journal of Mechanical Sciences*, Vol. 44, No. 10, pp.2089–2102.
- Hilditch, T.B. and Hodgson, P.D. (2005) 'Development of the sheared edge in the trimming of steel and light metal sheet: Part 1-experimental observations', *Journal of Materials Processing Technology*, Vol. 169, No. 2, pp.184–191.
- Husson, C., Correia, J. P. M., Daridon, L. and Ahzi, S. (2008) 'Finite elements simulations of thin copper sheets blanking: study of blanking parameters on sheared edge quality', *Journal of Materials Processing Technology*, Vol. 199, No. 1, pp.74–83.
- Jin, S., Wang, X., Du, L. and He, D. (2021) 'Evaluation and modeling of automotive transmission whine noise quality based on MFCC and CNN', *Applied Acoustics*, Vol. 172, p.107562.
- Li, X. and Bassiuny, A.M. (2008) 'Transient dynamical analysis of strain signals in sheet metal stamping processes', *International Journal of Machine Tools and Manufacture*, Vol. 48, No. 5, pp.576–588.
- Liu, X., Pei, D., Lodewijks, G., Zhao, Z. and Mei, J. (2020) 'Acoustic signal based fault detection on belt conveyor idlers using machine learning', *Advanced Powder Technology*, Vol. 31, No. 7, pp.2689–2698.
- Mei, Q., Gül, M. and Boay, M. (2019) 'Indirect health monitoring of bridges using mel-frequency cepstral coefficients and principal component analysis', *Mechanical Systems and Signal Processing*, Vol. 119, pp.523–546.
- Niaki, F.A., Feng, L., Ulutan, D. and Mears, L. (2016) 'A wavelet-based data-driven modelling for tool wear assessment of difficult to machine materials', *International Journal of Mechatronics and Manufacturing Systems*, Vol. 9, No. 2, pp.97–121.
- Picart, P., Makich, H., Carpentier, L., Monteil, G., Roizard, X. and Chambert, J. (2008) 'Metrology of the burr amount – correlation with blanking operation parameters (blanked material – wear of the punch)', *International Journal of Material Forming*, Vol. 1, No. S1, pp.1243–1246.
- Zhai, G., Chen, J., Li, C. and Wang, G. (2015) 'Pattern recognition approach to identify loose particle material based on modified MFCC and HMMs', *Neurocomputing*, Vol. 155, pp.135–145.
- Zhu, K.P., Wong, Y.S. and Hong, G.S. (2009) 'Wavelet analysis of sensor signals for tool condition monitoring: a review and some new results', *International Journal of Machine Tools and Manufacture*, Vol. 49, Nos. 7–8, pp.537–553.